Rotational elastic micro joint based on helix-augmented cross-spring design for large angular movement

Cheol Woo Ha and Dong-Yol Yang*

Department of Mechanical Engineering, Korea Advanced Institute of Science & Technology (KAIST), Science Town, Daejeon, 305-701, South Korea

*dyyang@kaist.ac.kr

Abstract: A new type of micro-joint based on an elastic design concept is proposed for large rotational movement. The proposed new 3D micro-joint was designed based on a cross-spring that has precise and reliable motion. However, the cross-spring has a limitation in the range of rotational angle. To improve the range of rotational movement, the proposed 3D micro-joint was modified with a helical structure. By adding the helical structure, the modified rotational joint can achieve large rotational movement The micro-joint was fabricated by the two-photon stereolithography process (TPS process). The micro-joint was manipulated by optical trapping force. With the same optical trapping force, the advantage of proposed cross-spring on the large rotational movement was evaluated. And the precise movement of the proposed micro-joint was evaluated by calculating the RMS error. It has been shown that the proposed 3D micro-joint has precise and reliable motion for large rotational angle.

OCIS codes: (350.4855) Optical tweezers or optical manipulation; (190.4180) Multiphoton processes; (230.4000) Microstructure fabrication; (230.4685) Optical microelectromechanical devices.

References and links

1. E. Higurashi, O. Ohguchi, T. Tamamura, H. Ukita, and R. Sawada, "Optically induced rotation of dissymmetrically shaped fluorinated polyimide micro-objects in optical traps," J. Appl. Phys. **82**(6), 2773–2779 (1997).
2. S. Maruo, "Light-driven MEMS made by high-speed two-photonmicrostereolithography," in *14th IEEE Conference on Micro Electro Mechanical Systems* (2001), pp. 594–597.
3. P. Galajda and P. Ormos, "Rotors produced and driven in laser tweezers with reversed direction of rotation," Appl. Phys. Lett. **80**(24), 4653–4655 (2002).
4. S. Maruo, K. Ikuta, and H. Korogi, "Force-controllable, optically driven micromachines fabricated by single-step two-photon micro stereolithography," J. Microelectromech. Syst. **12**(5), 533–539 (2003).
5. S. Maruo and H. Inoue, "Optically driven micropump produced by three-dimensional two-photon microfabrication," Appl. Phys. Lett. **89**(14), 144101 (2006).
6. S. Maruo and H. Inoue, "Optically driven viscous micropump using a rotating microdisk," Appl. Phys. Lett. **91**(8), 084101 (2007).
7. H. Xia, J. A. Wang, Y. Tian, Q. D. Chen, X. B. Du, Y. L. Zhang, Y. He, and H. B. Sun, "Ferrofluids for fabrication of remotely controllable micro-nanomachines by two-photon polymerization," Adv. Mater. **22**(29), 3204–3207 (2010).
8. Y. J. Jeong, T. W. Lim, Y. Son, D. Y. Yang, H. J. Kong, and K. S. Lee, "Proportional enlargement of movement by using an optically driven multi-link system with an elastic joint," Opt. Express **18**(13), 13745–13753 (2010).
9. C. L. Lin, Y. H. Lee, C. T. Lin, Y. J. Liu, J. L. Hwang, T. T. Chung, and P. L. Baldeck, "Multiplying optical tweezers force using a micro-lever," Opt. Express **19**(21), 20604–20609 (2011).
10. H. B. Sun, K. Takada, and S. Kawata, "Elastic force analysis of functional polymer submicron oscillators," Appl. Phys. Lett. **79**(19), 3173–3175 (2001).
11. H. Z. Zhao and S. Bi, "Stiffness and stress characteristics of the generalized cross-spring pivot," Mechanism Mach. Theory **45**(3), 378–391 (2010).
12. H. Z. Zhao and S. S. Bi, "Accuracy characteristics of the generalized cross-spring pivot," Mechanism Mach. Theory **45**(10), 1434–1448 (2010).

#213905 - $15.00 USD Received 11 Jun 2014; revised 18 Jul 2014; accepted 18 Jul 2014; published 20 Aug 2014

13. Z. He, H. Qian, D. Wu, W. Wang, X. Liu, and J. C. Liu, "Design of flexural pivot for use in hard disc drive actuator," Microsyst. Technol. **9**(6–7), 453–460 (2003).
14. D. Y. Yang, S. H. Park, T. W. Lim, H. J. Kong, S. W. Yi, H. K. Yang, and K. S. Lee, "Ultraprecise microreproduction of a three-dimensional artistic sculpture by multipath scanning method in two-photon photopolymerization," Appl. Phys. Lett. **90**(1), 013113 (2007).
15. T. W. Lim, Y. Son, D. Y. Yang, H. J. Kong, K. S. Lee, and S. H. Park, "Highly effective three-dimensional large-scale microfabrication using a continuous scanning method," Appl. Phys. A-Mater. **92**(3), 541–545 (2008).
16. R. Guo, S. Xiao, X. Zhai, J. Li, A. Xia, and W. Huang, "Micro lens fabrication by means of femtosecond two photon photopolymerization," Opt. Express **14**(2), 810–816 (2006).
17. J. Serbin, A. Ovsianikov, and B. Chichkov, "Fabrication of woodpile structures by two-photon polymerization and investigation of their optical properties," Opt. Express **12**(21), 5221–5228 (2004).
18. W. H. Wright, G. J. Sonek, and M. W. Berns, "Parametric study of the forces on microspheres held by optical tweezers," Appl. Opt. **33**(9), 1735–1748 (1994).

1. Introduction

The mechanical actuators used in machinery, electronics, and biotechnology are composed of various types of joints. For micro-sized actuators, several types of micro-joints have been developed. These joints can be classified into two types according to whether they are based on a kinematic [1–7] or an elastic design [8–10]. The conventional micro-sized rotational joint is based on a kinematic design, such as a pin joint. However, for a pin joint, there must be clearance between the hole at the rotating arm and the pin to rotate the rotating arm freely, and this tolerance induces motion errors. In order to reduce these errors, the clearance between the fixed and moving parts should be smaller. This, however, gives rise to the problem of friction. On the micro/nano scale, the friction force is one of the dominant factors hindering the movement of the joint. Therefore, an elastic design that does not involve any kinematic clearance is more suitable for precise the movement of micro-joints.

Among the many elastic joints available, the cross-spring is one of the most precise rotational joints. It can be applied in various fields which require precise rotational motion [11–13]. Structurally, the cross-spring is composed of two orthogonally crossed thin plates that can link fixed and moving parts. Because the cross-spring is structured in an integrated joint, there is no clearance. The moving part can be rotated only with the elastic deformation of the two crossed thin plates. This makes it possible to realize reliable rotational movement with minimal motion error. In addition, the center of rotation is nearly fixed, and the rotational movement of the cross-spring thus maintains almost a constant radius during rotation. Therefore, the rotational joint based on a cross-spring structure can achieve highly precise rotational movement within limited small angle of rotation, for example, less than ten degrees. However, due to its high rotational stiffness, the cross-spring has a small amount of rotational movement and has a limitation in widening its applications to micro devices.

In this paper, to obtain a large angle of rotational movement covering tens of degrees for various applications of micro devices, a new concept of a micro-joint combining a cross-spring with a helical structure is proposed. When the helical structure is added, the elastic deformation for rotational movement can be increased to a great extent. This allows greater elastic deformation and a larger rotational angle compared to the conventional cross-spring. Furthermore, by increasing the number of turns of the helical structure, it becomes possible to improve the rotational angle of the cross-spring when combined with a helical structure.

The micro-rotational joint was fabricated using a two-photon stereolithography process. By applying optical trapping force, we demonstrate that the proposed joint has precise and reliable motion with a large range of rotational movement.

#213905 - $15.00 USD Received 11 Jun 2014; revised 18 Jul 2014; accepted 18 Jul 2014; published 20 Aug 2014

2. Experimental system

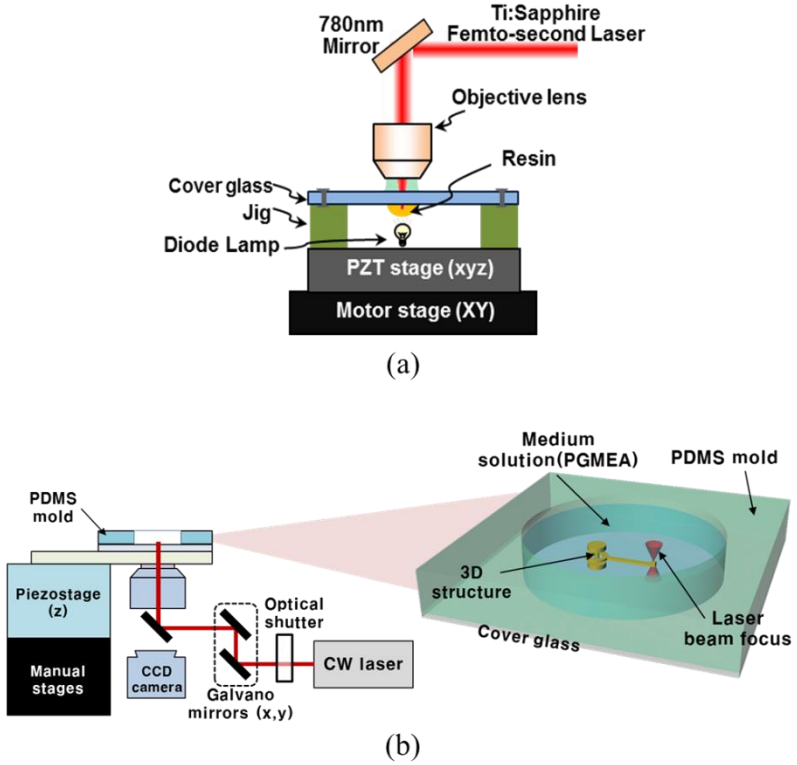

Fig. 1. Schematic diagrams of (a) the two-photon stereolithography system for 3D movable micro structures, and (b) the optical manipulation system for manipulation of the 3D movable structure.

A schematic diagram of the two-photon stereolithography (TPS) system for the fabrication of 3D micro-structures is shown in Fig. 1(a). The proposed micro rotational joint can be fabricated by using the two-photon stereolithography process. The TPS process is used for fabrication of 3D microstructures [14–17]. For the two-photon absorption process, a mode-locked Ti:sapphire laser with a wavelength of 780 nm was used as the laser source. An optical shutter for controlling the on/off state of the laser beam was operated. The laser beam was fixed and tightly focused by a high-numerical-aperture objective lens (N.A. 1.3, x 100 with immersion oil). A cover glass with photo-curable resin was fixed by a jig and was moved by controlling the x, y, and z directions via computer-controlled piezoelectric stages. For the photo-curable resin, SU8 (Micro Chem Corp.) was employed.

Figure 1(b) shows the optical manipulation system used to manipulate the movable structure. The polydimethylsiloxane (PDMS) fixed on the cover glass has a cavity at the center position. Propylene glycol monomethyl ether acetate (PGMEA) was used as the SU8 developer to eliminate the uncured region of SU8 and fill in the cavity. The fabricated SU8 was developed in the cavity. After the developing process, the rotational joint was fixed on a glass filled with a PGMEA solution. To generate optical trapping force, a continuous-wave laser was used in the optical trapping system. For precise manipulation of the 3D movable structure, a Galvano scanning mirror with a high resolution and a high response time was used. A high magnification charge-coupled-device (CCD) camera was operated to obtain real-time vision image during the manipulation process. The Ti:sapphire laser was focused on the optical trapping point. Because the refractive index of the 3D movable structure is higher than

#213905 - $15.00 USD Received 11 Jun 2014; revised 18 Jul 2014; accepted 18 Jul 2014; published 20 Aug 2014

that of the medium, optical trapping force was generated on the 3D movable structure (refractive index of SU8 = 1.5; refractive index of PGMEA = 1.4).

3. Measurement of the optical trapping force

For manipulation of 3D micro-joints with proper optical trapping force, it is important to measure the optical trapping force according to the various laser power. There are several methods for the measuring the optical trapping force. One of the method for the measuring the optical trapping force was the method using drag force [18]. The micro-sphere beads were driven by optical trapping force in the fluid solution with the viscosity (μ). The optical trapping force is determined by the escape velocity when the micro-sphere beads moves with the laser beam. And it is not require consideration of any material properties of the bead.

In this paper, the micro-be ads in a PGMEA solution was were driven by the optical trapping force. The radius (R) of a micro-sphere bead was 3μm, and the viscosity (μ) of PGMEA solution was 0.8 mPa·s. The Ti:sapphire laser (λ = 780nm) was focused at on the micro-beads using an the objective lens (N.A. 1.4, x 100 with immersion oil). Using the CCD camera, the escape velocity (V) was obtained. The velocity was increased by in given increments by increasing the laser power. For the calculation of the optical trapping force, the values of the viscous drag force were calculated using the Stoke's law, as expressed in Eq. (1).

$$F_D = 6\pi\mu RV \tag{1}$$

Figure 2 shows the relationship between the laser power and the optical trapping force as calculated by Eq. (1). The optical trapping force is proportional to the intensity of the laser power. In this work, the laser power at 500mW was used for the manipulation of the micro rotational joint. For a laser power at 500mW, the optical trapping force (F_D) was calculated to be 68pN

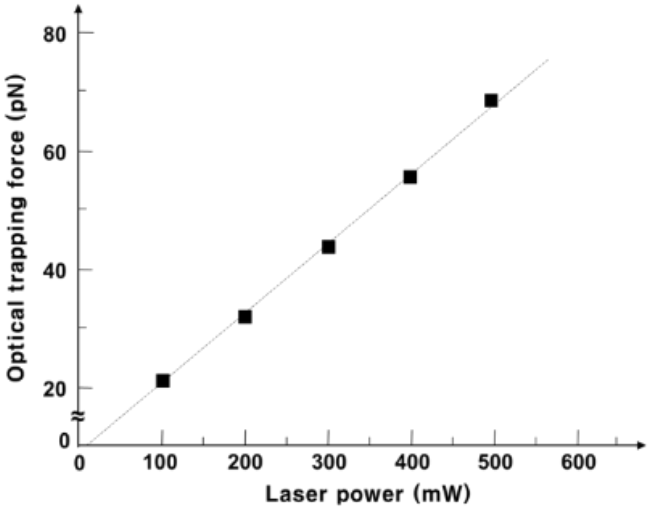

Fig. 2. Calculation of the optical trapping force versus the laser power.

#213905 - $15.00 USD Received 11 Jun 2014; revised 18 Jul 2014; accepted 18 Jul 2014; published 20 Aug 2014

4. Elastic beam for a micro-rotational joint

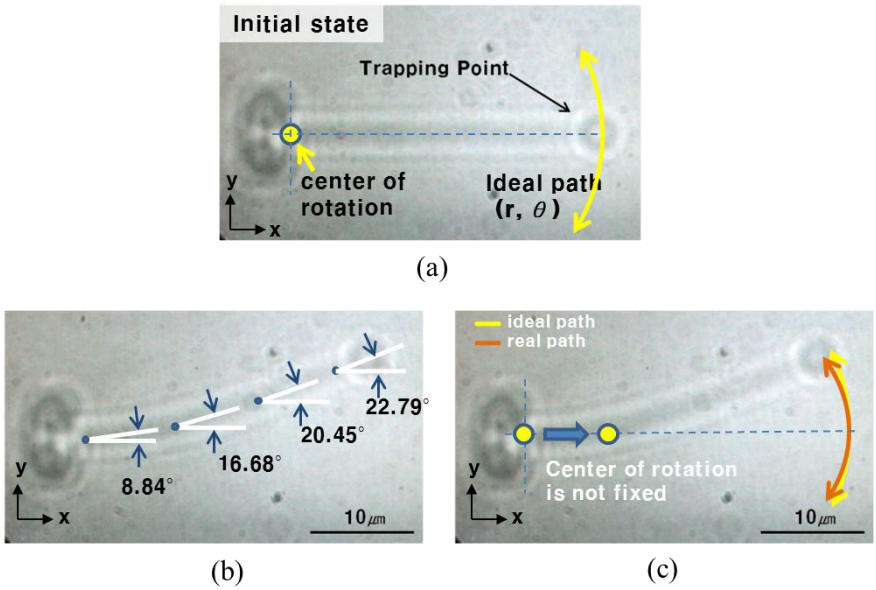

Fig. 3. CCD images show the cantilever beam at (a) the initial state and (b, c) the maximum deformed state (see Media 1).

Rotational joints at the micro scale are generally designed using kinematic concepts. Kinematic designs have the benefit of free rotational movement, but they also have the limitation of inaccurate movement. For example, the kinematic design called a pin-joint, has a clearance between the hole at a rotating arm and a pin. Due to this clearance, the rotating arm does not move along the desired path; therefore, it is difficult to rotate it reliably in a controlled manner. When the rotational joint is designed using an elastic design concept, the rotational joint can be designed as an integrated structured. Because this form of joint rotates without any clearance, the motion error due to the clearance would be negligible; allowing the elastic rotational joint to be moved reliably along a fixed path of motion. Therefore, elastic rotational joints can inherently produce more reliable movement than rotational joints based on kinematic design.

A simple rotational joint based on an elastic design has an elastic beam shape [Fig. 3(a)]. The experimental elastic beam fabricated by the TPS process was 30 μm in length; with an optical trapping point located at its tip. The elastic beam was rotated using a CW laser scanned by a galvano scanning mirror. However, an elastic beam with an elastic rotational joint involve some problems. First, as the elastic deformation got larger, the deformation energy required, increased geometrically. Therefore, it was difficult to obtain the desired large deformation for the given amount of force.

Furthermore, for precise rotation, the center of rotation should be fixed and the rotational joint should be rotated with a constant radius of rotation with respect to the center of rotation [Fig. 3(b)]. However, when rotating the elastic beam from the initial state to the final state, each stepwise position of the elastic beam had a different interval of rotational angle. This is because the rotational angle becomes larger as the measurement point is approached to the tip of the elastic beam. The center of rotation is then not fixed and the trajectory of the elastic beam is not exactly circular [Fig. 3(c)]. Therefore, the elastic beam has a small rotational angle and is not suitable for accurate rotational motion. The goal for the new micro rotational joint based on an elastic design was to achieve both a large amount of rotational angle and precise circular rotational movement.

#213905 - $15.00 USD Received 11 Jun 2014; revised 18 Jul 2014; accepted 18 Jul 2014; published 20 Aug 2014

5. New design of the elastic joint: cross-spring

In order to overcome the problems discussed above, a new design concept for a rotational joint was proposed using a cross-spring based on an elastic design.

Cross-springs are widely used to achieve precise rotational movement [11–13]. As shown in Figs. 4(a) and 4(b), the two orthogonally-crossed thin plates connect the fixed and moving parts of the cross-spring. The cross-spring can be assembled to form an integrated structure based on an elastic design. The moving part can rotate precisely due to elastic deformation of the two, crossed thin plates. Because there is no clearance such as in a kinematic design, the cross-spring moves along a fixed rotational path without any motion error. When the cross-spring is rotating, it has an almost constant radius of rotation because the center of rotation is located at the intersection of the two thin plates. Therefore, a rotational joint using a cross-spring would provide reliable, accurate rotational movement.

Figure 4(c) shows the cross-spring as fabricated by TPS. The gap (g) between two thin plates was 1μm. The length (L) of each thin plate was 20 μm, and the cross-section dimensions are 0.5 μm in width (w) and 2μm in height (h). Because the cross-section of the thin plate has a high aspect ratio, it is cannot easily be deformed in the z-direction. Thus, the motion error due to deformation in the z-direction is negligible. The cross-spring was manipulated using an optical manipulation system. The driving speed of the laser was 4.02 μm/s. With the laser power at 500 mW, the maximum rotational angle of the cross-spring was 14.3° [Fig. 4(d)]. This result showed that it was not suitable for large rotational movement due to its small range of rotational angle.

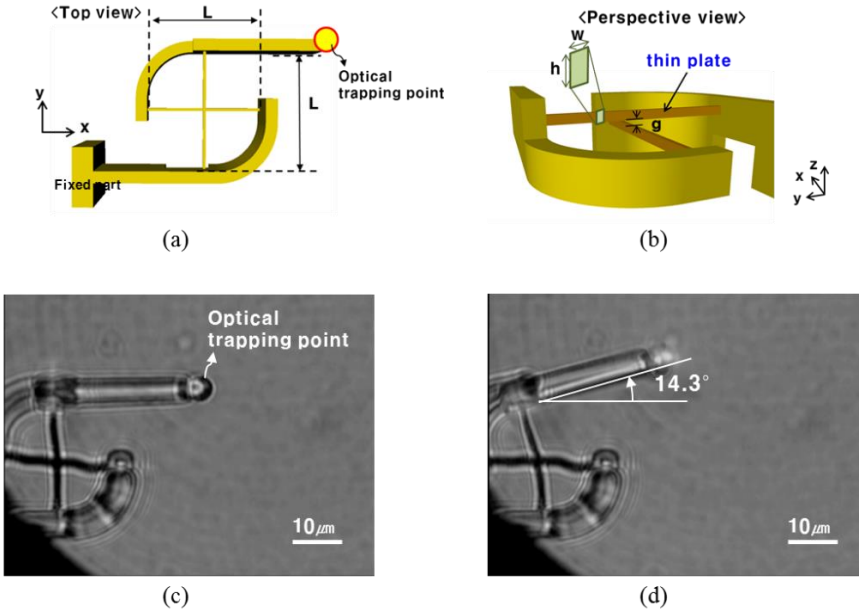

Fig. 4. Schematic diagram of the cross-spring based on an elastic design: (a) Top view and (b) Perspective view of the cross-spring; CCD images of the cross-spring at: (c) the initial-state, and (d) the maximum deformed state (see Media 2).

6. Modified design of the elastic joint: helix-augmented cross-spring

Due to the small range of rotational angle of the conventional cross-spring, its applicability for the rotational movement to various actuators would be limited. To improve the range of the rotational angle, a modified cross-spring was designed combining it with a helical structures. Figures 5(a) and 5(b) show the modified design of the elastic joint with one turn of the helical structure and two turns of the helical structure, respectively. A helical structure

#213905 - $15.00 USD Received 11 Jun 2014; revised 18 Jul 2014; accepted 18 Jul 2014; published 20 Aug 2014

was added to the middle of each thin-plate. When the helical structures are added, the total curvilinear length of the structure that can be elastically deformed becomes longer, and the rotational deformation should thus be increased. This can be explained through a comparison with the stiffness of helical structures with different numbers of turns.

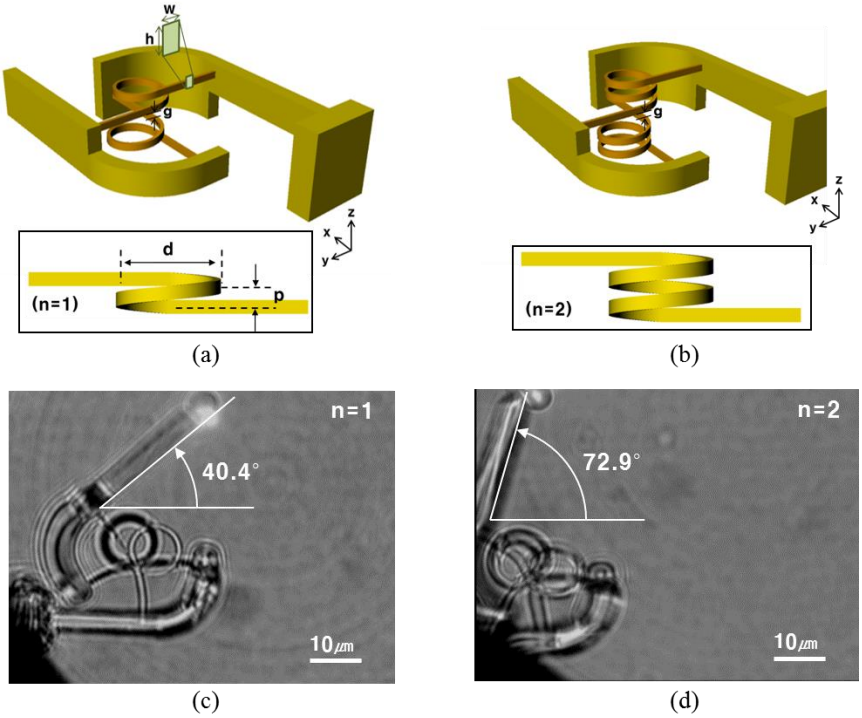

Fig. 5. Schematic diagram of the helix-augmented cross-spring: Perspective view of the cross-spring with (a) one turn of the helical spring and (b) two turns of the helical spring; CCD images of the maximum deformed state of helix-augmented cross-spring with the added helical structure with: (c) one turn (see Media 3), and (d) two turns (see Media 4).

Equation (2) shows the stiffness formula of the helical structure. In the equation, n is the number of turns of the helical structure with connection of a single turned helical structure (n = 1). k_c is the rotational stiffness of the conventional cross-spring, k_s is the rotational stiffness of a single turned helical structure and k is the rotational stiffness of the overall structure. The overall rotational stiffness can be expressed as Eq. (3). When the helical structure is added (n>0), the rotational stiffness of the overall structure (k) is less than that of the conventional cross-spring. When force (F) is applied to drive the rotational joint, the angular deformation (θ) of the rotational joints can be expressed as shown in Eq. (4). As the number of turns of the helical structure is increased, the value of k becomes smaller. Therefore, from Eq. (4), the amount of rotational deformation of the elastic rotational joint is increased.

$$\frac{1}{k} = \frac{1}{k_c} + \left(\frac{n}{k_s}\right)_{upper\ spring} + \left(\frac{n}{k_s}\right)_{bottom\ spring} = \frac{1}{k_c} + \frac{2n}{k_s} \tag{2}$$

$$k = k_c \frac{1}{1 + 2n(k_c / k_s)} \tag{3}$$

$$F = k\theta \tag{4}$$

#213905 - $15.00 USD Received 11 Jun 2014; revised 18 Jul 2014; accepted 18 Jul 2014; published 20 Aug 2014

Thus, by adding the helical structure to the conventional cross-spring (called helix-augmented cross-spring), it is expected that the rotational deformation would be larger. The helix-augmented cross-spring fabricated by the TPS process was then manipulated using the optical manipulation system. The driving speed of the laser was 4.02 μm/s. Figure 5(c) show the maximum rotational angle of the helix-augmented cross-spring with one turn of the helical structure. Figure 5(d) shows the maximum rotational angle of the helix-augmented cross-spring with two turns of the helical structure. The maximum rotational angle was 14.3° at n = 0 [Fig. 4(d)]. And the maximum rotational angle was 40.4° at n = 1, and 72.9° at n = 2. Therefore, as the number of turns of the helical structure is increased, the amount of rotational angle is increased. The helix-augmented cross-spring with two turns was able to rotate 5.1 times the angle of a conventional cross-spring.

7. Evaluation of precise movement of rotational-joints

To evaluate the precise movement of the rotational joint, the experimental results were compared to those of a simple cantilever beam and with cases of different numbers of turns of the helical structure. The rotational joints were rotated by a laser at 500 mW with a driving speed of 4.02μm/s. As shown in Figs. 6(a) and 6(b), the position of the optical trapping point was measured. The target trajectory is a circular path with a fixed radius (30μm).

As shown in Fig. 6(c), the elastic beam and cross-spring was rotated along the target trajectory. It was shown that the range of the rotational angle of an elastic beam has small amount of rotational angle. The helix augmented cross-spring has a large amount of rotational angle. Therefore, the helix augmented cross-spring is beneficial to large rotational movement at the micro-scale.

With the optical image from the CCD camera, the position error between the actual and target paths was measured, and the root-mean-square (RMS) error was calculated. Using the value of RMS error, the precise movement of rotational-joint can be evaluated. The RMS error (σ) of the cross-spring is much less than that of the simple elastic joint. This result shows that the cross-springs are more suitable for precise large rotational movement than the conventional elastic joints.

In case of the elastic joint, the RMS error of the elastic joint becomes significantly large as the rotational angle increases. Because each position of the elastic beam has a different instantaneous rotational angle during the rotation of the elastic joint, the center of the rotation is not fixed and the trajectory of the elastic joint is not basically circular. As discussed in section 4, the center of rotation should be fixed and the rotational joint should be rotated with a constant radius of rotation for precise rotation.

In case of the helix augmented cross-spring, the RMS error also grows with more turns of the helical structure. This occurs because the center line of the helical structure is not fixed. Therefore, with more turns of the helical structure, the stability (at a large rotational angle) decreases and the initial path has error according to the target path. However, the RMS error is saturated at a small RMS value as the rotational angle increases. Because the helix augmented cross spring is rotated based on the cross-spring movement, the advantage of a cross-spring is to keep the center of rotation almost fixed. Therefore, the center of rotation of the helix augmented cross-spring is almost fixed at the intersection of the two thin plates. And the helix augmented cross-spring is rotated precisely with almost constant radius of rotation.

#213905 - $15.00 USD Received 11 Jun 2014; revised 18 Jul 2014; accepted 18 Jul 2014; published 20 Aug 2014

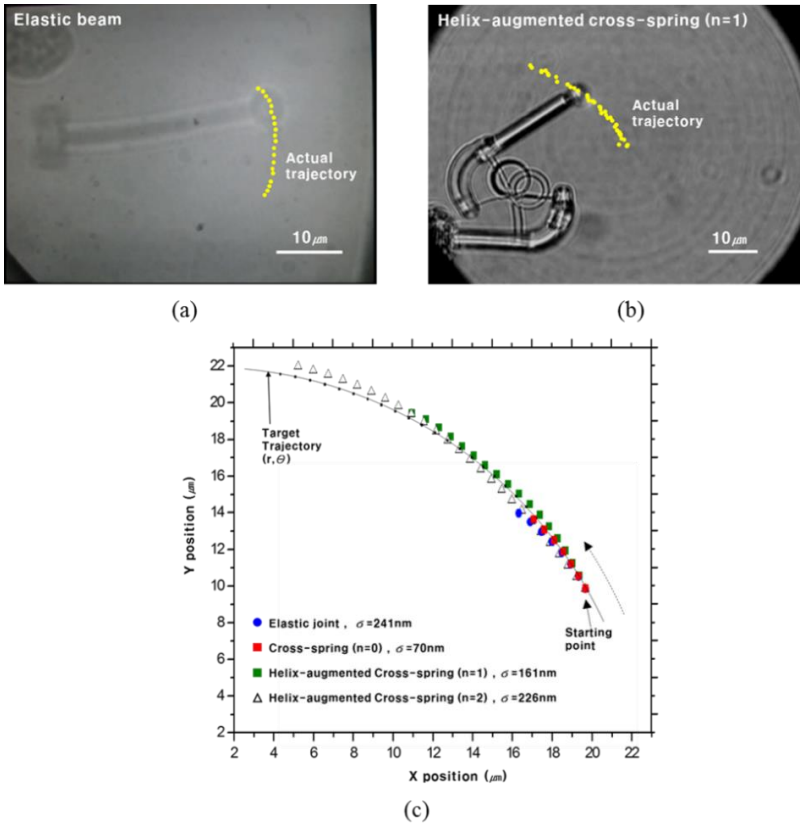

Fig. 6. Actual trajectory of (a) elastic beam and (b) helix-augmented cross-spring. (c) Moving accuracy of the rotational joint compared to the target trajectory.

8. Conclusions

In order to achieve precise rotational movement, a new design of a micro-rotational joint is proposed for precise and reliable rotational movement based on a cross-spring design which incorporates helical structures. With simple equations, it has been found out that the helix-augmented cross-spring can rotate more than a conventional cross-spring without any helical structure. The cross-spring was fabricated by using the two-photon stereolithography system and was manipulated by the optical trapping system. It has been demonstrated that the range of rotational movement can be increased as the number (n) of turns of the helical structure is increased. As compared to the rotational angle of the conventional cross-spring (n = 0), the helix-augmented cross-spring with n = 2 provides 5.1 times the rotational angle. In comparison with the actual trajectory to the circular target trajectory, it was found that the movement of the cross-spring is more accurate than the movement of a simple elastic joint.

It has been found that the proposed micro-rotational joint, helix-augmented cross-spring overcomes the limitations (e.g., motion error and small range of rotational movement) of existing micro-rotational joints. Since the helix-augmented cross-spring has been shown to provide precise, reliable movement; it has a good potential for use in a variety of complex applications such as cell manipulators and fluidic devices.

Acknowledgments

This study was supported by the Nano R&D program through the National Research Foundation of Korea funded by the Ministry of Science, ICT and Future Planning (2013R1A1A2005388).

#213905 - $15.00 USD Received 11 Jun 2014; revised 18 Jul 2014; accepted 18 Jul 2014; published 20 Aug 2014